Available at www.sciencedirect.com

ScienceDirect

journal homepage: www.elsevier.com/locate/he

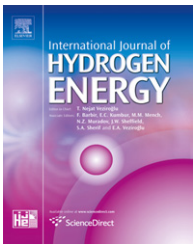

Review

Corrosion of metal bipolar plates for PEM fuel cells: A review

Renato A. Antunes [a,*], *Mara Cristina L. Oliveira* [b], *Gerhard Ett* [b], *Volkmar Ett* [b]

[a] *Engenharia de Materiais, Universidade Federal do ABC (UFABC), 09210-170 Santo André, SP, Brazil*
[b] *Electrocell Ind. Com. Equip. Elet. LTDA, Centro de Inovação, Empreendedorismo e Tecnologia (CIETEC), 05508-000 São Paulo, SP, Brazil*

ARTICLE INFO

Article history:
Received 28 September 2009
Received in revised form
13 January 2010
Accepted 18 January 2010
Available online 13 February 2010

Keywords:
PEM fuel cells
Metal bipolar plates
Corrosion
Stainless steel
Coatings

ABSTRACT

PEM fuel cells are of prime interest in transportation applications due to their relatively high efficiency and low pollutant emissions. Bipolar plates are the key components of these devices as they account for significant fractions of their weight and cost. Metallic materials have advantages over graphite-based ones because of their higher mechanical strength and better electrical conductivity. However, corrosion resistance is a major concern that remains to be solved as metals may develop oxide layers that increase electrical resistivity, thus lowering the fuel cell efficiency. This paper aims to present the main results found in recent literature about the corrosion performance of metallic bipolar plates.

1. Introduction

The global climate changes produced by greenhouse gases emissions such as CO_2, NO_x and SO_x that are ongoing throughout the world pose a progressively higher demand for replacing today's fossil fuel based energy production by less pollutant technologies [1,2]. Among the alternative energies available proton exchange membrane (PEM) fuel cells have been considered to power transportation vehicles such as automobiles and buses due to their high power density, relatively quick start-up, low operating temperatures and low greenhouse gas emissions [3]. All main vehicle manufacturers like General Motors, Ford, Toyota and Peugeot are developing fuel cell cars. Honda launched the first commercial fuel cell car, the FCX Clarity, in the United States market during 2008 summer [4]. Nevertheless, to completely achieve the automotive industry requirements PEM fuel cells have to overcome some intrinsic limitations mainly related to durability and cost compared to conventional internal combustion engines [5].

The main components of a PEM fuel cell structure are bipolar plates and the membrane electrode assembly (MEA). The MEA comprises the proton exchange membrane, gas diffusion layer (GDL) and a catalyst layer. A schematic view of such structure is shown in Fig. 1.

In a fuel cell stack the bipolar plates are key elements as they account for large fractions of the total weight, volume and cost of the stack. According to Tsuchyia and Kobayashi [6] bipolar plates may reach up to 80% of the total weight and 45% of the total cost in a PEM fuel cell stack. More recent data show that the relative cost has fallen to about 25% of the stack [7], yet a very significant amount. Furthermore these components

* *Corresponding author*. Tel.: +55 11 30398322; fax: +55 11 30398337.
E-mail address: renato.antunes@ufabc.edu.br (R.A. Antunes).
0360-3199/$ – see front matter © 2010 Professor T. Nejat Veziroglu. Published by Elsevier Ltd. All rights reserved.
doi:10.1016/j.ijhydene.2010.01.059

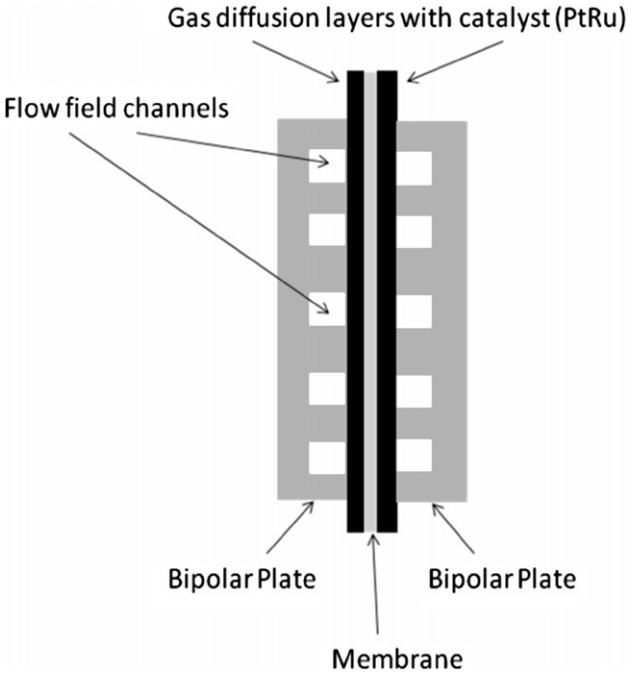

Fig. 1 Schematic view of a PEM fuel cell structure.

play vital functions in the stack such as to carry electric current away from each cell, to distribute fuel and oxidant homogeneously within individual cells, to separate individual cells and to facilitate the water management within the cell [8]. To perform such a number of functions a variety of materials have been proposed to the manufacturing of bipolar plates. The main properties that any material must present to be used in these devices are well established by the United States Department of Energy (DOE) as shown in Table 1. The criteria shown in this table are must-pass technical requirements that any material should be capable of achieving in order to be considered apt to a bipolar plate material.

The earlier traditional option was the use of non-porous graphite plates due to their intrinsic high electrical conductivity and chemical stability in the PEM fuel cell aggressive environment. Although the performance of graphite plates are suitable related to these properties they are brittle and lack mechanical resistance. Another drawback is the need for machining the flow field channels which raises the manufacturing cost making it prohibitive for mass production [9].

Table 1 Performance requirements for PEM fuel cell bipolar plates.

Property	Unit	Value
Tensile strength – ASTM D638	MPa	>41
Flexural strength – ASTM D790	MPa	>59
Electrical conductivity	S cm^{-1}	>100
Corrosion rate	μA cm^{-2}	<1
Contact resistance	mΩ cm^2	<20
Hydrogen permeability	cm^3 (cm^2 s)$^{-1}$	<2.10^{-6}
Mass	kg/kW	<1
Density – ASTM D792	g cm^{-3}	<5
Thermal conductivity	W (m K)$^{-1}$	>10
Impact resistance (unnotched) ASTM D-256	J m^{-1}	>40,5

Alternatives to pure graphite plates are composite bipolar plates based on the mixture of polymers and graphite particles. This class of materials allows mass production at a reasonable cost using manufacturing processes such as injection molding for thermoplastics or BMC for thermosets. There are several examples of graphite-based composite bipolar plates using polypropylene (PP), polyphenylene sulfide (PPS), phenolic and vinyl ester resins as matrices [10–14]. The polymer matrix gives flexibility to the bipolar plate improving its mechanical strength. The chemical stability is also not badly affected by the incorporation of polymer in graphite. On the other hand, electrical conductivity is proportionally diminished since polymers are insulating materials. Thus it is mandatory to formulate a composite bipolar plate with careful to attain mechanical performance without sacrifice electrical conductivity.

In spite of all the advantages of graphite-based composite bipolar plates regarding to their low weight, high production and chemical stability, if one compares their overall performance with that of metal bipolar plates two major drawbacks become evident, that is, their lower mechanical resistance and electrical conductivity. Considering especially transportation applications metal bipolar plates are more resistant to mechanical shocks and vibrations that could lead to cracking and leaking of reactant gases. Cunningham [15] presented data showing that the electrical conductivity of metal bipolar plates may reach up to 1000 times that of composite ones. In addition, they present easy manufacturability at low cost which increases their competitiveness in the fuel cell market [16]. However, a significant handicap that may decrease metal bipolar plates' performance is the susceptibility to corrosion in the acid and humid environment of PEM fuel cells. Metals operating in the fuel cell with a pH of 2–4 and temperatures around 80 °C may suffer dissolution. The ions leached may poison the membrane electrode assembly (MEA), decreasing the power output of the fuel cell [17,18]. Furthermore, passive layers formed during operation increase the electrical resistivity of metal bipolar plates. Consequently, the fuel cell efficiency is also negatively affected due to the raising of interfacial contact resistance as the oxide layer grows. These effects offset the advantage of high electrical conductivity [19].

The problems outlined above may be overcome or minimized by protecting metal bipolar plates from the corrosive fuel cell operating conditions with coatings [20]. A wide variety of alternatives have been proposed in research works towards this objective. This paper aims to present major research topics and results in the corrosion protection and characterization of metal bipolar plates for PEM fuel cells. Different coating methods and substrate materials are addressed giving a comprehensive overview on this subject.

2. Review

2.1. *Stainless steels*

2.1.1. *Bare substrates*

It is generally agreed that stainless steels are prone to chemical attack in the PEM fuel cell environment. Their corrosion

products may poison the catalysts in the polymeric membrane and the oxide layer grown on the metal surface increases the interfacial contact resistance decreasing the power output of the fuel cell [21]. The criterion to select stainless steels for bipolar plate applications sharply depends on the chemical composition of the material as the nature and content of alloying elements strongly influence the composition of the passive film formed on the metal surface which in turn affects its overall corrosion resistance. Hornung and Kappelt [22] used the pitting resistance equivalent (PRE = %Cr + 3.3*x* %Mo + 30*x*%N) to rank and select different iron-based materials for bipolar plates. The authors compared the performance of these alloys with nickel-based and gold-coated iron-based alloys. The alloys composition was not given in the text. Only the gold-coated alloy presented suitable contact resistance. Kim et al. [23] have also investigated stainless steels contact resistance for eleven different alloys exposed to sulfuric acid solution to simulate PEM fuel cell environment. They showed extensive results joining PRE numbers with transpassive potentials and contact electric resistance (CER) values. Chromium and molybdenum contents were found to be decisive for decreasing CER values. The authors outlined especially the molybdenum influence on PRE numbers, with a remarkable role for decreasing contact resistance of stainless steels passive films. The results were obtained from room temperature measurements only. In a real PEM fuel cell environment the operation temperature is in the range of 60 °C–80 °C. The corrosion rate of stainless steels increases as temperature raises [24] which may affect the passive layer composition and, hence, contact resistance. Kim et al. disregarded this feature on their work. So, the contact resistance values showed in the paper should be envisaged mainly as revealing a tendency related to the influence of Cr and Mo contents and not as absolute true values in a real PEM fuel cell device.

Silva et al. [25] pointed out the strong influence of the oxide film composition on the electrical conductivity of stainless steels passive layer. They studied the corrosion and interfacial contact resistances of 304, 310 and 316L stainless steels and four different nickel-based alloys regarding their suitability to operate in a PEM fuel cell environment.

Davies et al. [26] tested three different non-coated austenitic stainless steels, namely, 316, 310 and 904L grades. The corrosion resistance was dependent on the alloying content on the material. Grade 904L that presents the highest chromium and nickel contents showed the lowest contact resistance. According to the authors all the alloys presented high corrosion resistance in the fuel cell environment, similar to graphite bipolar plates during long term tests. Conversely, Hodgson et al. [27] showed that 316 stainless steel presented poor performance in fuel cell environment. This behavior was related to the increase in contact resistance as a result of the thickening of the oxide layer on the material surface. Makkus et al. [28] tested seven different non-coated stainless steels and found that, whatever the composition, all the materials showed poor resistance to corrosive attack. These findings corroborate Hentall et al. [29] that found bare 316L to be unsuitable for bipolar plate purposes also due to an increase in contact resistance during exposure to the fuel cell environment. Similar results have been found by other authors [17,19,30]. Iversen [31] investigated the corrosion behavior of austenitic, duplex and high molybdenum stainless steels with regard to bipolar plate applications. Among twelve materials tested the author selected two possible candidates, the austenitic grade 904L and the duplex grade S32205. The high molybdenum grades and conventional grades like 316L were found to be unsuitable due to an increase of contact resistance with time. Furthermore, Iversen identified a beneficial effect of manganese addition to decrease the electrical resistance of stainless steels. He suggested a suitable combination of manganese and molybdenum additions to produce a high pitting resistant and electrical conductive stainless steel passive layer. The work of Wang et al. [17] compared the electrochemical behavior of 316L, 317L, 349™ and 904L stainless steel grades in simulating fuel cell anode and cathode environments. The authors related the Cr content with the corrosion and interfacial contact resistances of the material. The results pointed towards the following performance order 349™ >904L > 317 L > 316L. This order shows that the higher the Cr content the higher the corrosion resistance. It was verified that the thickness of the passive layer on the 349™ grade was constant with time when the material was polarized at 0.6V during 30 min. Obviously this period is too short for a definite and accurate conclusion. However the results clearly allowed stating that 349™ is the best candidate for bipolar plate applications. An important fact, not mentioned in Wang's paper is the influence of both nickel and molybdenum contents on the contact resistance of the passive films formed on stainless steels.

Kumagai et al. [32] studied the corrosion behavior of 310 and 304 stainless steels in an acidic electrolyte simulating the operative conditions of PEM fuel cells. They found that 304 grade was readily corroded while 310 presented high corrosion resistance according to potentiodynamic polarization curves. This result was ascribed to the formation of a stable passive film on the metal surface. However, the polarization results should not be considered individually as the formation of a stable passive film may increase the contact resistance, leading to a decrease in the power density generated by the fuel cell. Actually, the contact resistance values of 310 stainless reported by Kumagai et al. are far higher than the technical target of 10 mΩ cm^2 established by DOE. Pozio et al. [33] conducted potentiodynamic polarization tests with 304 and 316L stainless steels in simulating PEM fuel cell electrolyte. The corrosion current densities of both materials were found to be higher than the target of 1 μA cm^{-2}. In addition, the interfacial contact resistance was also unsuitable for bipolar plate applications in agreement with other authors [26–31]. A contrary conclusion was held by Shanian and Savadogo [34]. They considered and ranked twelve different metallic materials as candidates for bipolar plates. The selection criteria were based on mechanical, thermal and electrical properties. Additional parameters were corrosion resistance, hydrogen permeability, cost and recyclability. The authors evaluated five different austenitic stainless steels (304, 310, 316, 316L and 317L), four ferritic grades (434, 436, 444 and 446), gold coated aluminum, nitride coated titanium and a nickel-based alloy. According to the methodology used in the paper the two most suitable materials for bipolar plates were the austenitic stainless steels 316L and 316, respectively. These findings are

opposite to most results found in the literature. This discrepancy may be due to the fact that the authors did not consider the two main drawbacks of uncoated stainless steels when exposed to the fuel cell environment, i.e., the increasing of interfacial contact resistance and the releasing of metal ions that poison the membrane. These aspects have not been considered by the selection process, producing a misleading conclusion. Based on the literature findings it is clear that non-coated stainless steels almost always lack corrosion resistance leading to an increasingly poor performance in the fuel cell environment when used as bipolar plates. Therefore it is mandatory that some surface modification method or protective coating be applied on stainless steels in order to improve their performance against corrosion [35].

2.1.2. *Surface treatments*

Lee et al. [36,37] suggested an electrochemical surface treatment on stainless steel bipolar plates to improve their corrosion resistance and minimize the formation of a thick oxide layer that increases interfacial contact resistance during operation. The results showed an increase in the breakdown potential and a decrease in the corrosion current density after treatment. They ascribed this superior behavior to the Cr enrichment of the oxide layer as verified using electron spectroscopy analysis. No details on the composition of the electrolyte used to perform the electrochemical treatment were given in the text. Cho et al. [38] evaluated the corrosion resistance of chromized 316L in PEM fuel cell simulating conditions. The chromium layer was produced by a pack cementation process. The treatment was effective with regard to the improvement of corrosion resistance of bare 316L. The lowest values of current density as shown by potentiodynamic and potentiostatic tests were obtained for a 2.5h period of treatment. These results were due to a Cr-rich layer with few defects. In a more recent investigation [39], the same authors used another pack cementation process to produce corrosion resistant chromized 316L stainless steel bipolar plates. They varied the Cr content in the powder mix used for the Cr pack cementation and the heating time during the chromizing treatment. The microstructure of the chromized layer was found to be strongly related to these process parameters. The process with a longer heating period led to the formation of a thicker Cr-rich layer, which was also richer in oxygen and presented no signs of chromium carbides. The process with a shorter heating period, on the other hand, produced a thinner Cr-rich layer, less oxygen and the formation chromium carbide on the surface of the stainless steel. Both processes led to higher corrosion resistance in comparison with the untreated material. However, the interfacial contact resistance of the bare 316L stainless steel presented a 6-fold increase after the process with long heating time. Conversely, the process with a short cementation time was effective to decrease the contact resistance of the 316L stainless steel. The chromium carbide on the surface of the treated material was of prime importance to achieve a good performance. This article shows how the control of the parameters in the chromizing process is essential to the development of a suitable microstructure. Yang et al. [40] attained a marked improvement in the corrosion and contact resistances of 316L stainless steel after a chromizing surface treatment. They reported a decrease of up to four orders of magnitude in the corrosion rate while the contact resistance of the chromized material was only one third of that of the untreated one. Bai et al. [41] combined a chromizing treatment with electron discharge machining (EDM) to enhance the corrosion resistance and decrease the contact resistance of low carbon steel bipolar plates. The EDM process was used to control the surface roughness and to diminish the contact resistance of the treated material. The treated material was shown to achieve the technical requirements of DOE for corrosion and contact resistances. The presence of carbides and nitrides in the surface of the carbon steel after the chromizing treatment are related to this achievement. To our knowledge this is the only report on low carbon steels for PEM fuel cells bipolar plates in the literature. The contact resistance was even lower than that of a stainless steel bipolar plate tested for comparison.

Kim and Kim [42] added different amounts of W, Ta and La to an austenitic stainless steel. Potentiodynamic and potentiostatic polarization tests in simulating PEM fuel cell environment showed that the modified material presented no active–passive transition and a stable current density with no signs of pitting corrosion in comparison with the original unmodified stainless steel. The contact resistance was also decreased after the modification. The authors ascribed this behavior to the formation of a protective and conducting film of WO_3. Nikam et al. [43] proposed a low cost treatment for increasing the corrosion performance of 316 stainless steel bipolar plate. They carried out a low temperature carburization of 316 specimens, avoiding the precipitation of chromium carbides at grain boundaries that is known to deplete the intergranular corrosion resistance of stainless steels [44]. They found corrosion current densities of 4 $\mu A\ cm^{-2}$ and 0.5 $\mu A\ cm^{-2}$ at anode and cathode PEM fuel environments, respectively for the surface treated 316 specimens while the untreated material, on the other hand, presented values of 24.4 $\mu A\ cm^{-2}$ and 35.2 $\mu A\ cm^{-2}$, respectively. The formation of a thin oxide layer after carburization accounts for the improvement of both corrosion and interfacial contact resistance. Nam and Lee [45] have tested chrome plating followed by thermal nitriding to enhance the corrosion performance of 316L stainless steel bipolar plates. Cr_2N films grown by thermal nitriding on chromium plated surfaces have proved to be satisfactory in the PEM fuel cell environment, providing good corrosion resistance. Thermal nitriding of austenitic stainless steels was also carried out by Wang et al. [46]. The authors verified that nitrided 349™ stainless steel presented unacceptable high corrosion current densities in comparison with the original material and suggested that some modification of the nitriding process parameters such as time and temperature may be necessary to improve the corrosion resistance. In the light of these findings Lee et al. [47] proposed a pre-oxidation treatment before the thermal nitriding of a ferritic grade stainless steel bipolar plate. According to the authors, the pre-oxidation treatment avoids the formation of discontinuous external Cr-nitrides that causes the exposure of Cr-depleted regions to the corrosive electrolyte of the fuel cell. Thus, the corrosion resistance is raised. In spite of the good results presented in this article, when the corrosion behavior of the nitrided ferritic stainless steel is compared

with that of an austenitic grade treated in a similar way, the current densities are higher for the ferritic material. This should be considered for a long-term operation in the PEM fuel cell environment. Yang et al. [48], on the other hand, have found very promising corrosion properties for a nitrided V-modified Fe–27Cr alloy. The corrosion current densities of this material were more than one order of magnitude lower than that presented by a 316 stainless steel specimen tested under the same conditions. The improvement of the corrosion resistance was ascribed to the enhancement of external nitride layer formation due to vanadium additions. Tian et al. [49,50] performed electrochemical tests with low temperature plasma nitrided 316L and 304L bipolar plates. Nitriding of austenitic stainless steels at temperatures below 450 °C is known to produce a dense γ_N layer that presents high electrical conductivity and corrosion resistance [51]. Potentiodynamic polarization curves showed that after treatment the corrosion potential was shifted to nobler values and the corrosion current density decreased for both materials. Using X-ray diffraction they proved that CrN and Cr_2N phases were absent at the surface of the nitrided materials and verified that the only phase was γ_N. The presence of CrN and Cr_2N is related to a chromium depletion of the passive layer which, in turn, leads to a decrease of the corrosion resistance for austenitic stainless steels [51]. Hence, the structural features of the low temperature nitride layer obtained by Tian et al. should be the responsible for the high corrosion resistance of the treated materials. Corroborating these results Han et al. [52] also achieved high corrosion and low contact resistances for chromium electroplated 316L stainless steel bipolar plates after low temperature plasma nitriding.

Feng et al. [53,54] tried to improve the performance of 316L stainless steel bipolar plate using ion implantation to modify its passive layer composition. They used two different approaches. The first one was the implantation of only nickel ions [53] and the second one was the co-implantation of nickel and chromium ions [54]. In both cases the corrosion resistance was increased and the interfacial contact resistance decreased to the enrichment of nickel and/or chromium in the passive film. Nevertheless, the contact resistance values are still higher than the DOE target of 10 $m\Omega\ cm^2$. Despite this fact, in comparison with other surface modification methods such as nitriding or PVD coatings the values are very similar or even better (see Table 2).

2.1.3. *Coatings*

The use of corrosion resistant and high conductive coatings is another surface modification technique envisaged as a solution to the lack of corrosion resistance of metal bipolar plates. A physical vapor deposition (PVD) method was used by Li et al. [55] to deposit titanium nitride (TiN) coating on 316L stainless steel bipolar plate as an alternative to protect the materials against the corrosive electrolyte of PEM fuel cells. Potentiodynamic polarization curves showed that the corrosion current density and passive current density of 316L were both decreased after the deposition of TiN, while the corrosion potential was shifted to nobler values. Furthermore, no signs of pitting were identified in the coated 316L specimens while in the bare specimens the polarization curves presented a breakdown potential at around 700 mV_{SCE}. Despite the promising electrochemical performance of TiN-coated 316L one concern was pointed out by the authors. Using SEM they found that the coating was lost on small areas on the material surface after 1000 h of immersion under cathodic conditions and after 240 h of immersion under anodic conditions. Consequently larger substrate areas may be exposed to the electrolyte with the increase of immersion time. This behavior has been ascribed to the presence of intrinsic defects on the coating layer such as pinholes and macroparticles that are inherent to PVD techniques [56]. A SEM micrograph of a PVD TiN-coated 316LSS is presented in Fig. 2. The defects of PVD film are clearly seen in this image.

In order to avoid this effect Li et al. suggested changes in the deposition parameters to improve the coating quality. Cho et al. [57] have also found that TiN coating on 316 stainless steel substrate provided good electrochemical performance in the fuel cell environment. However, they identified a coating degradation phenomenon responsible for increasing the charge transfer resistance and, in addition, lowering the ionic conductivity of the membrane due to poisoning by Fe, Cr, Ni and Ti ions released by the 316 substrate and TiN coating. Wang and Northhwood [58] conducted potentiodynamic testes with TiN-coated 316L stainless steel specimens and verified a drastic decrease of the corrosion current density. On the other hand, under potentiostatic conditions there was a three-fold increase in the current density at cathode simulating operation. This behavior was related by the authors to pitting corrosion due to the penetration of electrolyte through coating defects. The same authors [59] evaluated a TiN-coated martensitic stainless steel bipolar plate and found that the corrosion rate was decreased by two orders of magnitude in comparison with the uncoated material. Jeon et al. [60] investigated the influence of N_2 gas pressure during the deposition process over the corrosion resistance of TiN-coated 316L stainless steel under simulating PEM fuel cell environment. They found marked differences in corrosion current density and charge transfer resistance values depending on the N_2 pressure. The variations were ascribed to the porosity of the coatings which were dependent on the N_2 pressure employed during the deposition process. The best performance was related to the coating with the lowest porosity percentage. This result was confirmed through SEM images of the coatings surfaces.

It is extensively documented that the presence of inherent defects on PVD coatings is a major concern as the corrosion resistance of the metal substrate is adversely affected by these imperfections [61–63]. In order to overcome these drawbacks other deposition processes have been tested on bipolar plate stainless steels. Myung et al. [64] applied TiN nanoparticles on 310S stainless steel via an electrophoretic deposition (EPD) process. Field emission SEM images showed that the nanoparticles were still covering the stainless steel surface after 300 h of a normal PEM fuel cell operation. As a consequence of this relative stability the corrosion current density and contact resistance of the coated material were low, similarly to pure graphite bipolar plates. Multi-layered PVD coatings are often reported as a way of achieving defect-free, corrosion resistant coated metal plates [65,66]. Based on these findings Ho et al. [67] performed corrosion tests with Ti/TiN and Ti/CrN coated 304 stainless steel bipolar plates. The coatings have

Table 2 Corrosion data of metal bipolar plates for PEM fuel cell according to the literature reported in this review.

Bipolar plate material	Coating/Surface modification	Electrolyte	Corrosion current density ($\mu A\ cm^2$)	Potentiostatic results	Contact resistance at 20 kg cm^{-2} ($m\Omega\ cm^2$)	Reference
316LSS	–	0.5 M H_2SO_4 at 70 °C O_2 bubbled	9.145	−0.7 $\mu A\ cm^{-2}$ at −0.1 V)	–	[30]
		0.5 M H_2SO_4 at 70 °C H_2bubbled	2.426	and 5 $\mu A.cm^{-2}$ at +0.6 V		
904LSS	–	1 wt% Na_2SO_4 solution	~0.01	–	–	[31]
316LSS	–		~0.01	–	–	
S32205	–		~0.5	–	–	
LDX 2101	–		~0.4	–	–	
310SS	–	pH 3.3 (0.05 M SO_4^{2-} + 2 ppm F^- at 80 °C)	~0.5	~0.08	~150	[32]
304SS	–	10^{-3} M H_2SO_4 + 1.5 × 10^{-4} M	0.48	–	–	[33]
304SS	CrN	HCl + 15 ppm HF	0.10	–	30 at 15 kg cm^{-2}	
316LSS	–		0.46	–	–	
316LSS	CrN		0.20	–	21 at 15 kg cm^{-2}	
316LSS	–	0.5 M H_2SO_4 at room	60	–	15	[36]
316LSS	Electrochemical treatment–non specified	temperature	15	–	11	
316LSS	–	0.5 M H_2SO_4 at 80 °C	23	Unstable	–	[38]
316LSS	Cr pack cementation		0.2	~10 $\mu A\ cm^{-2}$ at +0.6 V	–	
316LSS	–	1 M H_2SO_4 at 80 °C	~100	–	35.3 at 15 kg cm^{-2}	[39]
316LSS	Cr pack cementation (2.5 h at 1050 °C)		~1	–	17 at 15 kg cm^{-2}	
316LSS	Cr pack cementation (23 h at 1050 °C)		~1	–	233.5 at 15 kg cm^{-2}	
316LSS	–	0.5 M H_2SO_4 + 2 ppm F^-	2000[a]	–	45	[40]
316LSS	Cr pack cementation (3 h at 1100 °C)	at room temperature	0.3[a]	0.075 $\mu A.cm^{-2}$ at −0.1 V	17	
316LSS	Cr pack cementation (3 h at 900 °C)		0.3[a]	0.35 $\mu A\ cm^{-2}$ at −0.1 V	13	
Carbon steel AISI 1020	–	0.5 M H_2SO_4 at 25 °C	634	–	403.8 at 14.3 kg cm^{-2}	[41]
Carbon steel AISI 1020	Chromizing		1.24	–	39.0 at 14.3 kg cm^{-2}	
Carbon steel AISI 1020	EDM (2 A) + Chromizing		0.058	–	11.8 at 14.3 kg cm^{-2}	
16Cr–12Ni–4Mo	–	1 M H_2SO_4 + 2 ppm F^- at	15.8	0.5 $\mu A\ cm^{-2}$ at −0.1 V	75	[42]
18Cr-12Ni–2Mo–3W	–	80 °C, H_2 purge	11.2	0.2 $\mu A\ cm^{-2}$ at −0.1 V	90	
316SS	–	0.5 M H_2SO_4 + 2 ppm HF	24	–	125	[43]
316SS	Low temperature carburization	at 80 °C	2–4	4 $\mu A\ cm^{-2}$ at −0.1 V	100	
316LSS	–	0.5 M H_2SO_4 + 2 ppm HF	152	–	~84 at 15 kg cm^{-2}	[45]
316LSS	Nitrided Cr_2N	at 80 °C	0.58	0.2$\mu A\ cm^{-2}$ at −0.1 V	~66 at 15 kg cm^{-2}	
316LSS	Nitrided Cr_2N + CrN		4.99		~50 at 15 kg cm^{-2}	

(*continued on next page*)

Table 2 (*continued*).

Bipolar plate material	Coating/Surface modification	Electrolyte	Corrosion current density (μA cm^2)	Potentiostatic results	Contact resistance at 20 kg cm^{-2} (mΩ cm^2)	Reference
349SS	Nitridation	1 M H_2SO_4 + 2 ppm F^- at 70 °C O_2 bubbled	~1000	20 mA cm^{-2} at −0.1 V	9.5 at 18 kg cm^{-2}	[46]
349SS	Nitridation	1 M H_2SO_4 + 2 ppm F^- at 70 °C H_2 bubbled	~1000	0.25 mA cm^{-2} at +0.6 V		
446MSS	–	pH 3H_2SO_4 solution at 80 °C purged with H_2	100	6 μA cm^{-2} at −0.1 V	30 at 15 kg cm^{-2}	[47]
446MSS	Nitridation		2.0	–	7–8 at 15 kg cm^{-2}	
446MSS	Pre-oxidation + Nitridation		1.5	5–6 μA cm^{-2} at −0.1 V	7–8 at 15 kg cm^{-2}	
316SS	–	pH 3H_2SO_4 solution at 80 °C	0.4	–	~100	[48]
Fe–27Cr	Nitridation		0.04	–	~7	
Fe–27Cr–2V	Nitridation		0.04	–	–	
Fe–27Cr–6V	Nitridation		0.02	−6 μA cm^{-2} at +0.14 V	~6	
316LSS	–	pH 3H_2SO_4 + 2 ppm F^- at 25 °C	~8	–	~90	[49]
316LSS	Nitridation		~0.2	–	~10	
304LSS	–	0.05 M H_2SO_4 + 2 ppm F^- at 70 °C H_2bubbled	~100	–	~80	[50]
304LSS	Nitridation		~90	1.7 μA cm^{-2} at −0.1 V	~10	
316LSS	–	0.1 N H_2SO_4 + 2 ppm F^- at 80 °C H_2 bubbled	2.6	–	82 at 15 kg cm^{-2}	[52]
316LSS	Cr plating		0.025	–	–	
316LSS	Cr plating + Plasma Nitriding (−300 V)		−0.53	−0.1 μA cm^{-2} at −0.1 V	5.6 at 15 kg cm^{-2}	
316LSS	–	0.5 M H_2SO_4 + 2 ppm F^-at 80 °C	11.26	10 μA cm^{-2} at +0.6 V	312.8	[53]
316LSS	Ni ion implantation (1.10^{17} ions cm^{-2})		7.91 (passive current densities at +0.6 V)	1.3 μA cm^{-2} at +0.6 V	36	
316LSS	–	0.5 M H_2SO_4 + 2 ppm F^- at 80 °C, air bubbled	11.26	2.5–3.0 μA cm^{-2} at +0.6 V	255.4	[54]
316LSS	Cr–Ni co-ion implantation (2 h)		6.7	0.51 μA cm^{-2} at +0.6 V	22.1	
316SS	–	0.01 M HCl + 0.01 M Na_2SO_4 at 80 °C, H_2 bubbled	27.1	–	–	[55]
316SS	TiN (PVD)		0.32	−0.3 μA cm^{-2} at −0.24 V	–	
316LSS	–	0.5 M H_2SO_4 at 70 °C, H_2 bubbled	40.3	−10 μA cm^{-2} at −0.1 V	–	[58]
316LSS	TiN (PVD)		1.02	−40 μA cm^{-2} at −0.1 V	–	
410SS	–	0.5 M H_2SO_4 at 70 °C, air purged	189	Unstable at −0.1 V	–	[59]
410SS	TiN (PVD)		1.75	30 μA cm^{-2} at −0.1 V	–	
316LSS	–	1 M H_2SO_4 + 2 ppm F^- at 70 °C	57.0	–	–	[60]
316LSS	TiN (0.2 mTorr)		8.88	–	–	
316LSS	TiN (0.4 mTorr)		0.28	–	–	
316LSS	TiN (0.6 mTorr)		0.55	–	–	
310SS	–	0.05 M SO_4^{2-} + 2 ppm F^- at 80 °C	~1.0	~0.8 μA cm^{-2} at +0.6 V	550 after polarization at +0.6 V	[64]
310SS	TiN (EPD)		~0.5	~0.2 μA cm^{-2} at +0.6 V	10 after polarization at +0.6 V	

304SS	–	10% vol. H_2SO_4 solution at 80 °C	19.9	–	–	[67]
304SS	TiN	under continuous stirring	4.04	–	–	
304SS	CrN		0.64	–	–	
304SS	TiN/CrN		0.30	–	–	
304SS	CrN/Ti		0.50	–	–	
316LSS	–	0.5 M H_2SO_4 + 2 ppm HF at	4.76 (at +0.6 V)	–	80 at 15 kg cm^{-2}	[68]
316LSS	TiCrN (PVD); N_2 = 3 sccm	80 °C, air bubbled	0.49 (at +0.6 V)	0.1 μA cm^{-2} at +0.6 V	4.5 at 15 kg cm^{-2}	
304SS	–	0.5 M H_2SO_4 + 2 ppm HF at	~200	~80	–	[69]
304SS	Carbon (CVD)	80 °C, H_2 purged	~0.1	~10	–	
304SS	–	0.5 M H_2SO_4 + 2 ppm HF at	~600		–	
304SS	Carbon (CVD)	80 °C, O_2 purged	~0.05		–	
304SS	–	0.5 M H_2SO_4 at room temperature	~32	–	–	[71]
304SS	Carbon (CVD)		~8	–	–	
316LSS	–	0.5 M H_2SO_4 + 5 ppm HF at 25 °C	10	–	–	[72]
316LSS	C–Cr film (PBAIP)		0.1	–	6.86 at 15 kg cm^{-2}	
316LSS	–	0.5 M H_2SO_4 + 2 ppm HF at	43.1	2.4 μA cm^{-2} at +0.6 V	255.4	[73]
316LSS	Amorphous carbon film (PVD)	80 °C, air bubbled	0.06	2.8 μA cm^{-2} at +0.6 V	5.2	
316LSS	–	0.5 M H_2SO_4 + 5 ppm HF at 70 °C, H_2 purged	~400	–	–	[74]
316LSS	CrN	0.5 M H_2SO_4 + 5 ppm HF at 70 °C, H_2 purged	~2.0	–	5 at 15 kg cm^{-2}	
316LSS	–	0.5 M H_2SO_4 + 5 ppm HF at 70 °C, air purged	~316		–	
316LSS	CrN	0.5 M H_2SO_4 + 5 ppm HF at 70 °C, air purged	~0.8		–	
316LSS	–	0.5 M H_2SO_4 + 5 ppm HF at	320	1–10 μA cm^{-2} at +0.6 V	50 at 15 kg cm^{-2}	[75]
316LSS	CrN	70 °C, air bubbled	1–10	0.1–0.01 μA cm^{-2} at +0.6 V	8 at 15 kg cm^{-2}	
316LSS	–	0.5 M H_2SO_4 + 5 ppm HF at 25 °C	16 (at +0.6 V)	–	–	[76]
316LSS	CrN (PBAIP) (N content 0.5 %at.)		2.5 (at +0.6 V)	–	5.8 at 12 kg cm^{-2}	
304SS	–	1 M H_2SO_4 at room temperature	8.3	–	–	[77]
304SS	TiC		0.034	Steady state at 3.7 μA cm^{-2} after 4 h	–	
304SS	–	0.1 M H_2SO_4 (temperature	10	–	~80	[79]
304SS	PANI	non specified)	0.1	–	~580	
304SS	PPy		1	–	~500	
316LSS	–	0.5 M H_2SO_4 at 70 °C	40	5 μA cm^{-2} after 500 s (at +0.6 V)	–	[80]
316LSS	PPy		2.4	10 μA cm^{-2} after 2 h (at +0.6 V)	–	
316LSS	Gold interlayer; PPy top coating	0.5 M H_2SO_4 at 70 °C	5.46	−20 μA cm^{-2} (at −0.1 V) and 7 μA cm^{-2} (at +0.6 V)	–	[81]

(*continued on next page*)

Table 2 (*continued*).

Bipolar plate material	Coating/Surface modification	Electrolyte	Corrosion current density ($\mu A\ cm^2$)	Potentiostatic results	Contact resistance at 20 kg cm^{-2} ($m\Omega\ cm^2$)	Reference
304SS	–	0.1 M H_2SO_4 at 60 °C	5000	–	–	[82]
304SS	PPy		0.2	–	–	
430SS	Nb-cladding	1 M H_2SO_4 + 2 ppm HF at 80 °C, O_2 bubbled	0.0063		–	[84]
430SS	Nb-cladding	1 M H_2SO_4 + 2 ppm HF at 80 °C, H_2 bubbled	27	−10 $\mu A\ cm^{-2}$ (at −0.1 V)	8.5	
316LSS	–	1 M H_2SO_4 + 2 ppm F^- at	50	–	120	[85]
317LSS	–	70 °C, H_2 bubbled	11	–	–	
349SS	–		4	–	–	
316LSS	SnO_2:F		20	0.3 $\mu A\ cm^{-2}$ (at −0.1 V)	120	
317LSS	SnO_2:F		1	0.5 $\mu A\ cm^{-2}$ (at −0.1 V)	60	
349SS	SnO_2:F		1	1.5 $\mu A\ cm^{-2}$ (at −0.1V)	200	
441SS	–	1 M H_2SO_4 + 2 ppm F^- at	~1000	–	~100	[86]
444SS	–	70 °C, H_2 bubbled	~900	–	~60	
446SS	–		~8	–	~150	
441SS	SnO_2:F		~1000	10 $\mu A\ cm^{-2}$ (at −0.1 V)	~200	
444SS	SnO_2:F		~900	7.5 $\mu A\ cm^{-2}$ (at −0.1 V)	~170	
446SS	SnO_2:F		~0.3	−3.5 $\mu A\ cm^{-2}$ (at −.1 V)	~310	
444SS	SnO_2:F	1 M H_2SO_4 + 2 ppm F^- at	~1000	1 $\mu A\ cm^{-2}$ (at −0.1 V)	75	[87]
446SS	SnO_2:F	70 °C, H_2 bubbled	~30	−810 $\mu A\ cm^{-2}$ (at −0.1 V)	140	
434SS	–	1 M H_2SO_4 + 2 ppm F^- at	~1000	–	~50	[88]
436SS	–	70 °C, H_2 bubbled	~1000	–	~40	
441SS	–		~1000	–	~50	
444SS	–		~800	–	~40	
446SS	–		~7	2 $\mu A\ cm^{-2}$ (at −0.1 V)	~60	
6061 Al alloy	–	0.1 M H_2SO_4 (temperature	~10	–	~40	[93]
6061 Al alloy	PANI	non specified)	~10	–	~300	
6061 Al alloy	PPy		0.01	–	~1300	
316LSS	–	1 M H_2SO_4 + 2 ppm F^- at	~384	–	–	[94]
$Fe_{48}Cr_{15}Mo_{14}Y2C_{15}B_6$	–	75 °C, H_2 bubbled	~6	–	–	
$Fe_{50}Cr_{18}Mo_8Al_2Y_2C_{14}B_6$	–		~187	−25 $\mu A\ cm^{-2}$ (at −0.1 V)	–	
316LSS	–	1 M H_2SO_4 + 2 ppm F^- at	~350	–	~7	[95]
$Fe_{50}Cr_{18}Mo_8Al_2Y_2C_{14}B_6$	–	80 °C, H_2 bubbled	~150	–	~11	
$Fe_{43}Cr_{18}Mo_{14}C_{15}B_6Y_2Al_1N_1$	–		~20	–	~9	
$Ni_{60}Nb_{20}Ti_{10}Zr_5Ta_5$	–		~90	–	~13	
$Fe_{50}Cr_{18}Mo_8Al_2Y_2C_{14}B_6$	–	1 M H_2SO_4 + 2 ppm F^- at	~70	–	~12	[96]
$Fe_{41}Cr_{18}Mo_{14}C_{15}B_6Y_2N_4$	–	80 °C, H_2 bubbled	~20	–	~7	
316LSS	–	12.5 ppm H_2SO_4 + 1.8 ppm F^- at	0.087	–	–	[97]
$Zr_{75}Ti_{25}$	–	80 °C, H_2 bubbled	0.021	–	–	

C-17200 (Cu–Be alloy)	–	pH 3.26 (0.5 M H_2SO_4) at 70 °C	23.13	–	–	[99]
316LSS	–	pH 3 H_2SO_4 at 80 °C, air bubbled	9.28	–	25 at 15 kg cm^{-2}	[101]
Cu–5.3Cr	–		1520	–	<10 at 15 kg cm^{-2}	
Cu–5.3Cr	Nitridation		1480	1300 μA cm^{-2} at +0.6 V	<10 at 15 kg cm^{-2}	
Ni–Cr alloy	Nitridation	pH 3 H_2SO_4 at 80 °C	0.018	–	–	[102]

a Values of passive current density.

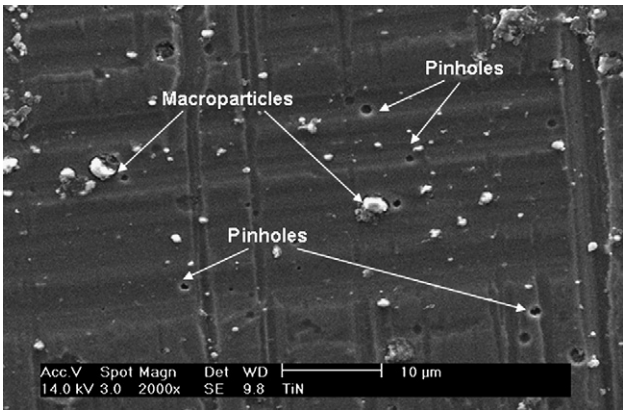

Fig. 2 SEM micrograph of a PVD-coated AISI 316L stainless steel showing pinholes and macroparticles in the film.

been deposited using a cathodic arc deposition system. The good corrosion resistance of the multi-layered coatings has been confirmed as the corrosion current densities were lower for the material coated with these coatings in comparison with the bare or single layer coated one. This behavior has been ascribed to the structure of the multi-layered coatings that inhibit the direct path between corrosive environment and the steel substrate. Choi et al. [68] showed that ternary (Ti,Cr)N_x coatings produced by inductively coupled plasma magnetron sputtering enhance the corrosion and electrical performance of 316L stainless steel in a simulated PEM fuel cell environment. The coating prevents the formation of oxygen on the surface of the material and act as an effective barrier between the substrate and the electrolyte. Fukutsuka et al. [69] used plasma assisted chemical vapor deposition process to produce a carbon layer on 304 stainless steel bipolar plate. The corrosion rate of the coated material was less than 1 μA cm^{-2} reaching therefore the US DOE technical target for bipolar plate [70]. Chung et al. [71] also evaluated the corrosion performance of a carbon coated 304 stainless steel bipolar plate. The carbon layer was produced via a chemical vapor deposition method using a C_2H_2/H_2 mixed gas as carbon source. Depending on the acetylene to hydrogen ratio the coating morphology varied from a filamentous porous layer to a continuous carbon coating. For the latter morphology the corrosion resistance was found to be high reaching the performance of commercial pure graphite bipolar plate (Poco graphite). Fu et al. [72] found that a C–Cr composite coating greatly decreased the interfacial contact resistance and corrosion rate of 316L stainless steel. They used a pulsed bias arc ion plating (PBDIP) deposition method which was chosen due to the low temperature, dense layer with few droplets that favor the final corrosion performance of the base metal. Feng et al. [73] investigated the performance of an amorphous carbon coated 316L stainless steel bipolar plate in a PEM fuel cell environment. They reported promising results of corrosion resistance under potentiodynamic and potentiostatic conditions and interfacial contact resistance. The dense and compact nature of the deposited film allied with the intrinsic high chemical stability and electrical conductivity of the carbon layer are responsible for the high desirable performance of the amorphous carbon coating. Fu et al. [74] considered the low-temperature deposition, reduced

droplets and dense films of PBDIP and produced a CrN coating layer on 316L stainless steel using this method. The values of corrosion current density for the coated specimens were smaller than those found for the base metal up to two orders of magnitude. This behavior was especially marked in the specimens that exhibited a surface coating layer composed of $Cr_{0.43}N_{0.57}$ that are said to be the most promising for commercial applications. The same approach was successfully undertaken by these authors in more recent publications [75,76]. The results confirmed the suitability of using a deposition process capable of achieving dense and compact films to protect metallic bipolar plates. Ren and Zeng [77] evaluated the electrochemical behavior of TiC coated 304 stainless steel bipolar plate in H_2SO_4 electrolyte. The coating layer was deposited through high-energy micro-arc alloying (HEMAA) technique that is known to produce pinhole-free, corrosion resistant coatings [78]. Potentiodynamic measurements showed that the corrosion resistance of the TiC coated material was far superior to that of bare 304. The corrosion current density for the coated steel was 0.0034 μA cm^{-2} while for the uncoated one the value was 8.3 μA cm^{-2}. Furthermore, the curve for the coated material presented no signs of pitting and a nobler corrosion potential. Electrochemical impedance spectroscopy results pointed out that the TiC coating was free of defects which accounts for its high corrosion resistance.

Conductive polymer coatings especially polypyrrole (PPy) and polyaniline (PANI) have been deposited on stainless steels bipolar plates in order to improve its corrosion resistance and increase electrical conductivity [79–82]. Joseph et al. [79] compared the electrochemical behavior of PPy and PANI-coated 304 stainless steel. It was found that both polymers decreased the corrosion current density of the bare material and shifted the corrosion potential to nobler values. However, the evolution of the electrochemical behavior was not accompanied with the immersion time. This information is crucial for a more reliable prediction of the bipolar plate candidate material behavior in simulating PEM fuel cell environment. Wang and Northwood [80] also reported low corrosion current density values for PPy-coated 316L. As in the work of Joseph et al. [79] they did not consider the coating degradation for long immersion times. They verified, however, that the metal ion concentration in solution was too high for PEM applications. So, regarding the improvement of PPy stability the same authors [81] deposited a nanothick gold interlayer between the 316L substrate and the polymer coating. This approach has led to a high corrosion resistant bipolar plate, presenting corrosion current density of 5.46 μA cm^{-2}. Though, other surface modification methods reported in the literature have produced a stainless steel bipolar plate with lower corrosion current density through simpler methods such as nitriding or a single coating layer [49,77]. García and Smit [82] also have found an excellent corrosion resistance for PPy-coated 304 stainless steel bipolar plates reaching corrosion current densities as low as 0.2 μA cm^{-2}. Nevertheless, they showed that the corrosion current density increased with time as a consequence of the disappearance of the coating layer as observed through SEM micrographs. It is clear, thence, that despite the suitable corrosion properties for short immersion times, PPy and PANI coatings lack stability for a well-succeeded commercial use as protective layers on stainless steel bipolar plates.

A different approach was developed by Kitta et al. [83]. They produced a conductive composite layer consisting of a carbon black/epoxy resin mixture that was applied on a 304 stainless steel substrate. The material maintained its corrosion resistance in air-humidified 95% RH (relative humidity) and 85 °C for 2000h and in 0.1M H_2SO_4 at 120 °C for 1200 h.

Another concept based on clad materials was undertaken by Weil et al. [84]. They developed Nb-clad 304 stainless steel bipolar plates owing to the corrosion resistance of Nb layer due to the formation an adherent native oxide film that passivates the metal substrate in acidic environments. It was found that the clad material was capable of achieving the DOE corrosion rate technical target of 1 μA cm^{-2}.

Wang et al. [85] have tested fluorine doped SnO_2 coating on austenitic stainless steels bipolar plates. This coating is known to be stable in aqueous solutions and is commonly used in photovoltaic industry owing to its high electrical conductivity. They found a decrease of the corrosion current density for F:SnO_2 coated 316L, 317L and 349 stainless steels in comparison with the bare materials. These authors have tried the same approach with the ferritic grades 441, 444 and 446 [86,87]. Depending on the pre-treatment of the material surface before the coating deposition the electrochemical behavior was markedly affected. When the authors used the same procedure employed for the austenitic grades [86] the results pointed towards similar results, i.e., after deposition of the F:SnO_2 layer the corrosion current density decreased one order of magnitude in comparison with the uncoated substrates. However, except for the 446 grade, the corrosion rates were too high even for the coated materials. The good corrosion resistance of 446 grade may be ascribed to its higher chromium and molybdenum content in comparison with 441 and 444 grades. Similar findings have been found for these substrates in another work of Wang and Turner [88]. When an etching process was employed before the coating deposition the corrosion resistance was decreased for all the ferritic grades tested [87]. This behavior was likely due to poor adhesion of the F:SnO_2 layer on the etched surface.

2.2. *Aluminum*

Aluminum may be considered for bipolar plate applications in PEM fuel cells due to the low manufacturing cost [89]. It is well propelled, though, that aluminum and its alloys do corrode in the fuel cell environment leaching ions that contaminate the membrane, decreasing the cell output [90,91]. Regardless this limitation, coated-aluminum bipolar plates may reach DOE technical targets [92]. Joseph et al. [93] found that PANI-coated 6061 Al alloy showed very good corrosion resistance compared to the uncoated substrate. The corrosion rate was up to 10^{-8} A cm^{-2} for a 40μm thick layer. However, no information about coating degradation in long-term immersion tests is reported in this paper. PPy coating, on the other hand, presented a corrosion current density of the same order of magnitude than that of the bare alloy. According to the authors the lack of corrosion resistance in this case was due to the pinholes on the polymer layer after deposition.

2.3. Amorphous alloys

Few reports on this subject are found in the technical literature. Jayaraj et al. [94,95] took into consideration the combination of properties such as superplasticity in the supercooled liquid region and high corrosion resistance of amorphous alloys to test these materials for PEM bipolar plate applications. They compared the corrosion resistance of the alloys $Fe_{48}Cr_{15}Mo_{14}Y_2C_{15}B_6$, $Fe_{44}Cr_{16}Mo_{16}C_{18}B_6$ and $Fe_{50}Cr_{18}Mo_8Al_2Y_2C_{14}B_6$ with that of conventional 316L stainless steel [94]. Potentiodynamic polarization curves showed that the corrosion rate of the amorphous alloys was related to their chromium content. The higher the chromium content the lower the corrosion rate. For the $Fe_{50}Cr_{18}Mo_8Al_2Y_2C_{14}B_6$ alloy the corrosion resistance was better than that of conventional 316L. This behavior could be due to the fact that grain boundaries in crystalline alloys act as potential sites for dissolution, increasing the corrosion rate. In spite of the relative low corrosion current density of the highest chromium amorphous alloy in comparison with 316L the value was too high if one takes into account the DOE target. Thus a bipolar plate made with this material would still need some surface modification method to improve its corrosion performance. Similar findings have been found by the same group for the amorphous alloys $Fe_{43}Cr_{18}Mo_{14}C_{15}B_6Y_2Al_1N_1$ and $Ni_{60}Nb_{20}Zr_{10}Ti_5Ta_5$ [95]. The positive influence of nitrogen addition on the corrosion resistance of Fe-based amorphous alloy was showed by the same group [96]. Jin et al. [97] have found better results for $Zr_{75}Ti_{25}$ bulk amorphous alloy with a corrosion current density of 0.021 $\mu A\ cm^{-2}$ under simulated anodic fuel cell environment after 5 h of immersion. There was no information, though, for longer immersion periods.

2.4. Copper alloys

Copper alloys have hardly been considered for bipolar plates of PEM fuel cells due to its high density. On the other hand, properties such as high electrical and thermal conductivity, chemical stability and easy manufacturing make these materials attractive for bipolar plates [98]. Nikam et al. [99,100] have investigated the corrosion resistance of C-17200 copper–beryllium alloy in simulated PEM fuel cell environment. The corrosion current density was dependent on the pH and temperature of the electrolyte. For the non-oxidizing anode medium the values at 70 °C were around 20 $\mu m\ cm^{-2}$ that are far superior to DOE current target of less than 1 $\mu m\ cm^{-2}$. Apparently, this alloy would not perform well during long term operation in the fuel cell environment. Lee et al. [101] studied the corrosion behavior of a nitrided Cu–5.3Cr alloy as PEMFC bipolar plate. They found that corrosion resistance in the cathode environment was too high for a suitable application as bipolar plate. The reason for the poor corrosion performance was the copper oxidation through pinholes in the nitrided layer. The susceptibility of copper alloys to corrosion in oxygen containing electrolytes is a serious drawback to its use as PEMFC bipolar plates.

2.5. Nickel and titanium alloys

Few corrosion investigations are found on nickel or titanium bipolar plates. The major drawback related to the use of these materials is the high cost. Nevertheless, Weil et al. [102] performed contact resistance measurements on boronized high purity nickel and commercial nickel-clad bipolar plates. Cladding an inexpensive core material like stainless steel with nickel plates may be an effective method to obtain a cheap and corrosion resistant component. The approach was based on the fact that transition metal borides offer a combination of high electrical conductivity and corrosion resistance. Although no corrosion properties have been reported in this paper, the authors stated that initial tests showed a dramatic increase in the corrosion resistance of the boronized materials in 80 °C 1 M H_2SO_4 + 2 ppm HF solution. Paulauskas et al. [103] investigated the corrosion behavior of nitrided Ni–50Cr bipolar plates and found corrosion current densities inferior to DOE target for specimens nitrided at 1100 °C during 2h under pure N_2 atmosphere.

Titanium based alloys have also been tested as potential bipolar plate materials for PEM fuel cells [104–106]. In all these reports the titanium plate is coated to protect it against the fuel cell electrolyte as the interfacial contact resistance of this material is prone to increase with time due to the formation of a stable oxide on its surface. Show [104] and Show et al. [105] evaluated the contact resistance of an amorphous carbon coated titanium bipolar plate. They did not assess the corrosion behavior of the coated materials but found good performance in single cell experiments and reduced contact resistance after the coating deposition. Wang et al. [106] found the same tendency for gold-plated titanium bipolar plates. However they did not report any result related to corrosion tests.

2.6. Effects of ion contamination on PEM fuel cell performance

Notwithstanding the crucial role of corrosion processes over the increase of the interfacial contact resistance of metal bipolar plates the effects of the resultant cationic contaminants on membrane conductivity should not be neglected. It is very probable that, in real PEM fuel cell systems, contaminants originated from several different sources poison the membrane decreasing the overall power output. Cheng et al. outlined all these sources of membrane contamination in a recent review paper [107]. Cationic impurities are released after corrosion of bipolar or end plates and even of the fuel cell piping system. Collier et al. [108] cited the presence of Fe^{3+}, Cu^{2+} and other cations in a unit cell MEA after 10,000 h of operation. According to Cheng et al. [107] almost all cations exhibit higher affinity for the sulfonic groups in the polymeric membrane than H^+. Hence, when other cations exchange for protons in the polymer structure, the amount of water in the cell is reduced.

Kelly et al. [109,110] investigated the influence of Fe^{3+}, Cu^{2+} and Ni^{2+} concentration (in ppm) on the Nafion membrane conductivity. A little effect was observed for up to 10 ppm of the ionic species. There was a huge drop of membrane conductivity when the cation concentration reached 100 ppm. This effect was most intense for Fe^{3+} contamination. This behavior was explained through Okada et al. [111] and Laconti et al. [112] findings. Okada et al. stated that membrane dehydration is caused by the lower hydrophilicity of impurity

cations when compared to H^+. Additionally, LaConti et al. showed that multivalent cations have higher affinity to sulfonic acid groups in the Nafion™ membrane than monovalent cations. The foreign ion displaces one H^+ for each charge on its structure. Consequently, its mobility is lower than that of H^+, accounting for a further decrease of ionic conductivity. This mechanism was depicted in a study of Shi and Anson [113]. They conducted a series of experiments with many different cations replacing protons in Nafion™ structure.

Another membrane degradation mechanism related to the presence of foreign was described in the work of Inaba et al. [114]. The deterioration was quantified by computing the fluoride release of the membrane under an open circuit potential condition. The authors detected hydrogen peroxide in the drain water of a PEM fuel cell. Hydrogen peroxide was produced at the anode catalyst as a result of combustion between adsorbed hydrogen and crossover oxygen from the cathode side. However, as pointed out in the paper, hydrogen peroxide was not the main responsible for Nafion™ degradation. Oxygen radicals formed upon decomposition of hydrogen peroxide in the presence of Fe^{2+} or Cu^{2+} ions were driven the degradation processes.

3. Conclusions

There is a wide variety of materials and surface modification methods available for metal bipolar plate development. It is evident that the major challenges regarding to a successful commercial use in PEM fuel cells are related to increasing corrosion resistance and decreasing contact resistance at a reasonable cost. Table 2 summarizes the literature findings on the corrosion data found on all the papers reported in this review. Few materials present a suitable combination of corrosion current density and contact resistance according to DOE targets. Depending on the reference consulted different values of corrosion current density have been found for the same material, especially for 316LSS. These values may vary as a function of electrolyte composition, pH and temperature, specimen surface finishing and small variations on the composition of the material itself. Although there is a plenty of information on the corrosion resistance of metal bipolar plates, long term results are often missing on most part of the literature reports. It must be considered too that even if the bipolar plate presents corrosion current density slightly higher than the DOE target of 1 $\mu A\ cm^{-2}$ it is not necessarily true that its behavior will not be acceptable during long term operation. The overall performance must take into account the fuel cell output which, in turn, depends also on interfacial contact resistance and contamination of the membrane with metal ions produced by the corrosion processes. The search for coatings or surface modification treatments that are capable of increasing bipolar plate corrosion resistance and simultaneously decrease contact resistance is a very well established trend. Interesting results have been reported on nitriding, PVD or CVD coatings and passive film modification. The main challenges are to produce defect-free coatings, stable passive films or nitride layers that are able to protect the metallic substrate from the fuel cell harsh environment.

4. Recommendations for future work

As described in the previous sections the corrosion behavior of metal bipolar plates may be improved with the modification of passive layer by incorporating elements capable of forming low resistance oxide films or the deposition of corrosion resistant coatings. In addition to these approaches recent investigations point towards an increase of the corrosion resistance of stainless steels after a surface treatment that promotes the formation of nanocrystalline grains [115–117]. The ultrafine microstructure would favor the migration of passivating elements to the material's surface. Thus, the corrosion resistance increases. The combination of this mechanism with the addition of alloying elements that tend to form a less resistive oxide layer such as tungsten [42] may produce a high corrosion resistant metallic bipolar plate. Furthermore, this approach may be combined with the deposition of protective coatings further enhancing the bipolar plate performance. None of these alternatives have been investigated in the literature.

Acknowledgement

The authors gratefully acknowledge FAPESP (The State of São Paulo Research Foundation) for the financial support.

REFERENCES

[1] Carrette L, Friedrich KA, Stimming U. Fuel cells – fundamentals and applications. Fuel Cells 2001;1(1):5–39.
[2] Collantes GO. Incorporating stakeholder's perspectives into models of new technologies diffusion: the case of fuel cell vehicles. Technol Forecasting Soc Change 2007;74(3):267–80.
[3] Schäfer A, Heywood JB, Weiss MA. Future fuel cell and internal combustion engine automobile technologies: a 25-year life cycle and fleet impact assessment. Energy 2006; 31(12):2064–87.
[4] Website, http://automobiles.honda.com/fcxclarity.
[5] Williams BD, Kurani KS. Commercializing light-duty plug-in/plug out hydrogen-fuel-cell vehicles: "Mobile Electricity" technology and opportunities. J Power Sources 2007;166(2): 549–66.
[6] Tsuchiya H, Kobayashi O. Mass production cost of PEM fuel cell by learning curve. Int J Hydrogen Energy 2004;29(10): 985–90.
[7] Samu A, Pertti K, Jari I, Pasi K. Bipolar plate, method for producing bipolar plate and PEM fuel cell. United State Patent Appl 20090142645; 2009.
[8] Cooper JS. Design analysis of PEMFC bipolar plates considering stack manufacturing and environment impact. J Power Sources 2004;129(2):152–69.
[9] Hermann A, Chaudhuri T, Spagnol P. Bipolar plates for PEM fuel cells: a review. Int J Hydrogen Energy 2005;30(12):1297–302.
[10] Müller A, Kauranen P, von Ganski A, Hell B. Injection molding of graphite composite bipolar plates. J Power Sources 2006;154(2):467–71.
[11] Radhakrishnan S, Ramanujam BTS, Adhikari A, Siravam S. High-temperature, polymer–graphite hybrid composites for bipolar plates: effect of processing conditions on electrical properties. J Power Sources 2007;163(2):702–7.

[12] Kakati BK, Deka D. Differences in physico-mechanical behaviors of resol(e) and novolac type phenolic resin based composite bipolar plate for proton exchange membrane (PEM) fuel cell. Electrochim Acta 2007;52(25):7330–6.
[13] Maheshwari PH, Mathur RB, Dhami TL. Fabrication of high strength and a low weight composite bipolar plate for fuel cell applications. J Power Sources 2007;173(1):394–403.
[14] Liao SH, Hung CH, Ma CHM, Yen. CY, Lin YF, Weng CC. Preparation and properties of carbon nanotube-reinforced vinyl ester/nanocomposite bipolar plates for polymer electrolyte membrane fuel cells. J Power Sources 2008; 176(1):175–82.
[15] Cunningham B. The development of compression moldable polymer composite bipolar plates for fuel cells. Thesis, Faculty of Virginia Polytechnic Institute and State University; 2007. p. 22–39.
[16] Tawfik H, Hung Y, Mahajan D. Metal bipolar plates for PEM fuel cell: a review. J Power Sources 2007;163(2):755–67.
[17] Wang H, Sweikart MA, Turner JA. Stainless steel as bipolar plate material for proton electrolyte membrane fuel cells. J Power Sources 2003;115(2):243–51.
[18] Pozio A, Silva R, De Francesco FM, Giorgi L. Nafion degradation in PEFCs from end plate iron contamination. Electrochim Acta 2003;48(11):1543–9.
[19] Wind J, Späh R, Kaiser W, Böhm G. Metallic bipolar plates for PEM fuel cells. J Power Sources 2002;105(2):256–60.
[20] Gamboa SA, Gonzalez-Rodriguez JG, Valenzuela E, Campillo B, Sebastian PJ, Reyes-Rojas A. Evaluation of the corrosion resistance of Ni–Co–B coatings in simulated PEMFC environment. Electrochim Acta 2006;51(19):4045–51.
[21] Kraytsberg A, Auinat M, Ein-Eli Y. Reduced contact resistance of PEM fuel cell's bipolar plates via surface texturing. J Power Sources 2007;164(2):697–703.
[22] Hornung R, Kappelt G. Bipolar plate materials development using Fe-based alloys for solid polymer fuel cells. J Power Sources 1998;72(1):20–1.
[23] Kim JS, Peelen WHA, Hemmes K, Makkus RC. Effect of alloying elements on the contact resistance and passivation behaviour of stainless steels. Corros Sci 2002;44(4):635–55.
[24] Hermas AA, Morad MS. A comparative study on the corrosion behaviour of 304 austenitic stainless steel in sulfamic and sulfuric acid solution. Corros Sci 2008;50(9):2710–7.
[25] Silva RF, Franchi D, Leone A, Pilloni L, Masci A, Pozio A. Surface conductivity and stability of metallic bipolar plate materials for polymer electrolyte fuel cells. Electrochim Acta 2006;51(17):3592–8.
[26] Davies DP, Adcock PL, Turpin M, Rowen SJ. Stainless steel as a bipolar plate material for solid polymer fuel cells. J Power Sources 2000;86(1–2):237–42.
[27] Hodgson DR, May B, Adcock PL, Davies DP. New lightweight bipolar plate system for polymer electrolyte membrane fuel cells. J Power Sources 2001;96(1):233–5.
[28] Makkus RC, Janssen AHH, Bruijn FA, Mallant RKAM. Use of stainless steel for cost competitive bipolar plates in the SPFC. J Power Sources 2000;86(1–2):274–82.
[29] Hentall PL, Lakeman JB, Mepsted GO, Adcock PL, Moore JM. New materials for polymer electrolyte membrane fuel cell current collectors. J Power Sources 1999;80(1–2):235–41.
[30] Wang Y, Northwood DO. Effects of O_2 and H_2 on the corrosion of SS316L metallic bipolar plate materials in simulated anode and cathode environments of PEM fuel cells. Electrochim Acta 2007;52(24):6793–8.
[31] Iversen AK. Stainless steels in bipolar plates – surface resistive properties of corrosion resistant steel grades during current loads. Corros Sci 2006;48(5):1036–58.
[32] Kumagai M, Myung ST, Kuwata S, Asaishi R, Yashiro H. Corrosion behavior of austenitic stainless steels as a function of pH for use as bipolar plates in polymer electrolyte membrane fuel cells. Electrochim Acta 2008; 53(12):4205–12.
[33] Pozio A, Zaza F, Masci A, Silva RF. Bipolar plate materials for PEMFCs: a conductivity and stability study. J Power Sources 2008;179(2):631–9.
[34] Shanian A, Savadogo O. TOPSIS multiple-criteria decision support analysis for material selection of metallic bipolar plates for polymer electrolyte fuel cell. J Power Sources 2006;159(2):1095–104.
[35] Li MC, Zeng CL, Luo SZ, Shen JN, Lin HC, Cao CN. Electrochemical corrosion characteristics of type 316 stainless steel in simulated anode environment for PEMFC. Electrochim Acta 2003;48(12):1735–41.
[36] Lee SJ, Huang CH, Lai JJ, Chen YP. Corrosion-resistant component for PEM fuel cells. J Power Sources 2004;131(1–2): 162–8.
[37] Lee SJ, Lai JJ, Huang CH. Stainless steel bipolar plates. J Power Sources 2005;145(2):362–8.
[38] Cho KH, Lee WG, Lee SB, Jang H. Corrosion resistance of chromized 316L stainless steel for PEMFC bipolar plates. J Power Sources 2008;178(2):671–6.
[39] Lee SB, Cho KH, Lee WG, Jang H. Improved corrosion resistance and interfacial contact resistance of 316L stainless steel for proton exchange membrane fuel cell bipolar plates by chromizing surface treatment. J Power Sources 2009;187(2):318–23.
[40] Yang L, Yu H, Jiang L, Zhu L, Jian X, Wang Z. Improved anticorrosion properties and electrical conductivity of 316L stainless steel as bipolar plate for proton exchange membrane fuel cell by lower temperature chromizing treatment. J Power Sources 2010;195(9):2810–4.
[41] Bai CY, Ger MD, Wu MS. Corrosion behaviors and contact resistances of the low-carbon steel bipolar plate with a chromized coating containing carbides and nitrides. Int J Hydrogen Energy 2009;34(16):6778–89.
[42] Kim KM, Kim KY. A new alloy design concept for austenitic stainless steel with tungsten modification for bipolar plate application in PEMFC. J Power Sources 2007; 173(2):917–24.
[43] Nikam VV, Reddy RG, Collins SR, Williams PC, Schiroky GH, Henrich GW. Corrosion resistant low temperature carburized SS 316 as bipolar plate material for PEMFC application. Electrochim Acta 2008;53(6):2743–50.
[44] Cao Y, Ernst F, Michal GM. Colossal carbon supersaturation in austenitic stainless steels carburized at low temperature. Acta Mater 2003;51(14):4171–81.
[45] Nam DG, Lee HC. Thermal nitridation of chromium electroplated AISI316L stainless steel for polymer electrolyte membrane fuel cell bipolar plate. J Power Sources 2007;170(2):268–74.
[46] Wang H, Brady MP, Teeter G, Turner JA. Thermally nitrided stainless steels for polymer electrolyte membrane fuel cell bipolar plates Part 1: model Ni–50Cr and austenitic 349TM alloys. J Power Sources 2004;138(1–2):86–93.
[47] Lee KH, Lee SH, Kim JH, Lee YY, Kim YH, Kim MC, et al. Effects of thermal oxi-nitridation on the corrosion resistance and electrical conductivity of 446M stainless steel for PEMFC bipolar plates. Int J Hydrogen Energy 2009; 34(3):1515–21.
[48] Yang B, Brady MP, Wang H, Turner JA, More KL, Young DJ, et al. Protective nitride formation on stainless steel alloys for proton exchange membrane fuel cell bipolar plates. J Power Sources 2007;174(1):228–36.
[49] Tian R, Sun J, Wang L. Plasma-nitrided austenitic stainless steel 316L as bipolar plate for PEMFC. Int J Hydrogen Energy 2006;31(13):1874–8.
[50] Tian R, Sun J, Wang L. Effect of plasma nitriding on behavior of austenitic stainless steel 304L bipolar plate in proton

exchange membrane fuel cell. J Power Sources 2007;163(2):719–24.
[51] Wang L. Surface modification of AISI 304 austenitic stainless steel by plasma nitriding. Appl Surf Sci 2003;211(1–4):308–14.
[52] Han DH, Hong WH, Choi HS, Lee JJ. Inductively coupled plasma nitriding of chromium electroplated AISI 316L stainless steel for PEMFC bipolar plate. Int J Hydrogen Energy 2009;34(5):2387–95.
[53] Feng K, Shen Y, Mai J, Liu D, Cai X. An investigation into nickel implanted 316L stainless steel as a bipolar plate for PEM fuel cell. J Power Sources 2008;182(1):145–52.
[54] Feng K, Shen Y, Liu D, Chu PK, Cai X. Ni–Cr co-implanted 316L stainless steel as bipolar plate in polymer electrolyte membrane fuel cell. Int J Hydrogen Energy 2010;35(2):690–700.
[55] Li M, Luo S, Zeng C, Shen J, Lin H, Cao C. Corrosion behavior of TiN coated type 316 stainless steel in simulated PEMFC environments. Corros Sci 2004;46(6):1369–80.
[56] Elsener B, Rota A, Böhni H. Impedance study on the corrosion of PVD and CVD titanium nitride coatings. Mater Sci Forum 1989;44–45:29–38.
[57] Cho EA, Jeon US, Hong SA, Oh IH, Kang SG. Performance of a 1 kW-class PEMFC stack using TiN-coated 316 stainless steel bipolar plates. J Power Sources 2005;142(1–2):177–83.
[58] Wang Y, Northwood DO. An investigation into TiN-coated 316L stainless steel as a bipolar plate material for PEM fuel cells. J Power Sources 2007;165(1):293–8.
[59] Wang Y, Northwood DO. An investigation of the electrochemical properties of PVDTiN-coated SS410 in simulated PEM fuel cell environments. Int J Hydrogen Energy 2007;32(7):895–902.
[60] Jeon WS, Kim JG, Kim YJ, Han JG. Electrochemical properties of TiN coatings on 316L stainless steel separator for polymer electrolyte membrane fuel cell. Thin Solid Films 2008;516(11):3669–72.
[61] Antunes RA. Thesis, University of São Paulo; 2006. p. 224–231.
[62] Yang D, Liu C, Liu X, Qi M, Lin G. EIS diagnosis on the corrosion behavior of TiN coated NiTi surgical alloy. Curr Appl Phys 2005;5(5):417–21.
[63] Liu C, Bi Q, Leyland A, Matthews A. An electrochemical impedance spectroscopy study of the corrosion behavior of PVD coated steels in 0.5 N NaCl aqueous solution. Part I: establishment of equivalent circuits for EIS data modeling. Corros Sci 2003;45(6):1243–56.
[64] Myung ST, Kumagai M, Asaishi R, Soon YK, Yashiro H. Nanoparticle TiN-coated type 310S stainless steel as bipolar plates for polymer electrolyte membrane fuel cell. Electrochem Commun 2008;10(3):480–4.
[65] Liu C, Leyland A, Bi Q, Matthews A. Corrosion resistance of multi-layered plasma assisted physical vapour deposition TiN and CrN coatings. Surf Coat Technol 2001;141(2–3):164–73.
[66] Nordin M, Herranen M, Hogmark S. Influence of lamellae thickness on the corrosion behaviour of multilayered PVD TiN/CrN coatings. Thin Solid Films 1999;348(1–2):202–9.
[67] Ho WY, Pan HJ, Chang CL, Wang DY, Hwang JJ. Corrosion and electrical properties of multi-layered coatings on stainless steel for PEMFC bipolar plate applications. Surf Coat Technol 2007;202(4–7):1297–301.
[68] Choi HS, Han DH, Hong WH, Lee JJ. (Titanium, chromium) nitride coatings for bipolar plate of polymer electrolyte membrane fuel cell. J Power Sources 2009;189(2):966–71.
[69] Fukutsuka T, Yamaguchi T, Miyano SI, Matsuo Y, Sugie Y, Ogumi Z. Carbon-coated stainless steel as PEFC bipolar plate material. J Power Sources 2007;174(1):199–205.
[70] DOE Hydrogen Program FY 2006 Annual Progress Report; 2006.p. 822.
[71] Chung CY, Chen SK, Chiu PJ, Chang MH, Hung TT, Ko TH. Carbon film-coated 304 stainless steel as PEMFC bipolar plate. J Power Sources 2008;176(1):276–81.
[72] Fu Y, Lin G, Hou M, Wu B, Shao Z, Yi B. Carbon-based films coated 316L stainless steel as bipolar plate for proton exchange membrane fuel cells. Int J Hydrogen Energy 2009;34(1):405–9.
[73] Feng K, Shen Y, Sun H, Liu D, An Q, Cai X, et al. Conductive amorphous carbon-coated 316L stainless steel as bipolar plates in polymer electrolyte membrane fuel cells. Int J Hydrogen Energy 2009;34(16):6771–7.
[74] Fu Y, Hou M, Lin G, Hou J, Shao Z, Yi B. Coated 316L stainless steel with CrxN film as bipolar plate for PEMFC prepared by pulsed bias arc ion plating. J Power Sources 2008;176(1):282–6.
[75] Fu Y, Lin G, Hou M, Wu B, Li H, Hao L, et al. Optimized Cr-nitride film on 316L stainless steel as proton exchange membrane fuel cell bipolar plate. Int J Hydrogen Energy 2009;34(1):453–8.
[76] Wu B, Fu Y, Xu J, Lin G, Hou M. Chromium nitride films on stainless steel as bipolar plate for proton exchange membrane fuel cell. J Power Sources 2009;194(2):976–80.
[77] Ren YJ, Zeng CL. Corrosion protection of 304 stainless steel bipolar plates using TiC films produced by high-energy micro-arc alloying process. J Power Sources 2007;171(2):778–82.
[78] Chen C, Wang M, Wang D, Jin R, Liu Y. Microstructure and corrosion behavior of Mg–Nd coatings on AZ31 magnesium alloy produced by high-energy micro-arc alloying process. J Alloys Compd 2007;438(1–2):321–6.
[79] Joseph S, McClure JC, Chianelli R, Pich P, Sebastian PJ. Conducting polymer-coated stainless steel bipolar plates for proton exchange membrane fuel cells (PEMFC). Int J Hydrogen Energy 2005;30(12):1339–44.
[80] Wang Y, Northwood DO. An investigation into polypyrrole-coated 316L stainless steel as a bipolar plate material for PEM fuel cells. J Power Sources 2006;163(1):500–8.
[81] Wang Y, Northwood DO. An investigation into the effects of a nano-thick gold interlayer on polypyrrole coatings on 316L stainless steel for the bipolar plates of PEM fuel cells. J Power Sources 2008;175(1):40–8.
[82] García MAL, Smit MA. Study of electrodeposited polypyrrole coatings for the corrosion protection of stainless steel bipolar plates for the PEM fuel cell. J Power Sources 2006;158(1):397–402.
[83] Kitta S, Uchida H, Watanabe M. Metal separators coated with carbon/resin composite layers for PEFCs. Electrochim Acta 2007;53(4):2025–33.
[84] Weil KS, Xia G, Yang ZG, Kim JY. Development of a niobium clad PEM fuel cell bipolar plate material. Int J Hydrogen Energy 2007;32(16):3724–33.
[85] Wang H, Turner JA, Li X, Bhattacharya R. SnO_2:F coated austenite stainless steels for PEM fuel cell bipolar plates. J Power Sources 2007;171(2):567–74.
[86] Wang H, Turner JA. SnO_2:F coated ferritic stainless steels for PEM fuel cell bipolar plates. J Power Sources 2007;170(2):387–94.
[87] Wang H, Turner JA, Li X, Teeter G. Process modification for coating SnO_2:F on stainless steels for PEM fuel cell bipolar plates. J Power Sources 2008;178(1):238–47.
[88] Wang H, Turner JA. Ferritic stainless steels as bipolar plate material for polymer electrolyte membrane fuel cells. J Power Sources 2004;128(2):193–200.
[89] El-Enim SAA, Abdel-Salam OE, El-Abd H, Amin AM. New electroplated aluminum bipolar plate for PEM fuel cell. J Power Sources 2008;177(1):131–6.
[90] Lee JH, Brady BK, Fuss RL. Corrosion resistant PEM fuel cell, United States Patent, 6,887,613; 2005.
[91] Lee SJ, Huang CH, Chen YP. Investigation of PVD coating on corrosion resistance of metallic bipolar plates in PEM fuel cell. J Mater Processing Technol 2003;140(1–3):688–93.

[92] Hung Y, El-Khatib KM, Tawfik H. Testing and evaluation of aluminum coated bipolar plates of PEM fuel cells operating at 70 °C. J Power Sources 2006;163(1):509–13.
[93] Joseph S, McClure JC, Sebastian PJ, Moreira J, Valenzuela E. Polyaniline and polypyrrole coatings on aluminum for PEM fuel cell bipolar plates. J Power Sources 2008;177(1):161–6.
[94] Jayaraj J, Kim YC, Kim KB, Seok HK, Fleury E. Corrosion studies on Fe-based amorphous alloys in simulated PEM fuel cell environment. Sci Technol Adv Mater 2005;6(3–4):282–9.
[95] Jayaraj J, Kim YC, Seok HK, Kim KB, Fleury E. Development of metallic glasses for bipolar plate application. Mater Sci Eng A 2007;449–451:30–3.
[96] Fleury E, Jayaraj J, Kim YC, Seok HK, Kim KY, Kim KB. Fe-based amorphous alloys as bipolar plates for PEM fuel cell. J Power Sources 2006;159(1):34–7.
[97] Jin S, Ghali E, Morales AT. Corrosion behavior of 316L stainless steel and $Zr_{75}Ti_{25}$ bulk amorphous alloy in simulated PEMFC anode environment in a solution containing 12.5 ppm H_2SO_4 + 1.8 ppm HF at 25 and 80 °C. J Power Sources 2006;162(1):294–301.
[98] Hsieh SS, Huang CF, Feng CL. A novel design and micro-fabrication for copper (Cu) electroforming bipolar plates. Micron 2008;39(3):263–8.
[99] Nikam VV, Reddy RG. Corrosion studies of a copper–beryllium alloy in a simulated polymer electrolyte membrane fuel cell environment. J Power Sources 2005;152(1):146–55.
[100] Nikam VV, Reddy RG. Copper alloy bipolar plates for polymer electrolyte membrane fuel cell. Electrochim Acta 2006;51(28):6338–45.
[101] Lee HY, Lee SH, Kim JH, Kim MC, Wee DM. Thermally nitrided Cu-5.3Cr alloy for application as metallic separators in PEMFCs. Int J Hydrogen Energy 2008;33(15):4171–7.
[102] Weil KS, Kim JY, Xia G, Coleman J, Yang ZG. Boronization of nickel and nickel clad materials for potential use in polymer electrolyte membrane fuel cells. Surf Coat Technol 2006; 201(7):4436–41.
[103] Paulauskas IE, Brady MP, Meyer III HM, Buchanan RA, Walker LR. Corrosion behavior of CrN, Cr_2N and π phase surfaces on nitrided Ni–50Cr for proton exchange membrane fuel cell bipolar plates. Corros Sci 2006;48(10):3157–71.
[104] Show Y. Electrically conductive amorphous carbon coating on metal bipolar plates for PEFC. Surf Coat Technol 2007; 202(4–7):1252–5.
[105] Show Y, Miki M, Nakamura T. Increased in output power from fuel cell used metal bipolar plate coated with a-C film. Diamond Relat Mater 2007;16(4–7):1159–61.
[106] Wang SH, Peng J, Lui WB, Zhang JS. Performance of the gold-plated titanium bipolar plates for the light weight PEM fuel cells. J Power Sources 2006;162(1):486–91.
[107] Cheng X, Shi Z, Glass N, Zhang L, Zhang J, Song D, et al. A review of PEM hydrogen fuel cell contamination: impacts, mechanisms and mitigation. J Power Sources 2007;165(2): 739–56.
[108] Collier A, Wang H, Yuan XZ, Zhang J, Wilkinson DP. Degradation of polymer electrolyte membranes. Int J Hydrogen Energy 2006;31(13):1838–54.
[109] Kelly MJ, Egger B, Fafilek G, Besenhard JO, Kronberger H, Nauer GE. Conductivity of polymer electrolyte membrane by impedance spectroscopy with microelectrodes. Solid State Ionics 2005;176(25–28):2111–4.
[110] Kelly MJ, Fafilek G, Besenhard JO, Kronberger H, Nauer GE. Contaminant absorption and conductivity in polymer electrolyte membranes. J Power Sources 2005;145(2):249–52.
[111] Okada T. Effect of ionic contaminants. In: Vielstich W, Gasteiger HA, Lamm A, editors. Handbook of fuel cells—fundamentals, technology and applications, vol. 3. John Wiley and Sons, Ltd; 2003. p. 627.
[112] LaConti AB, Hamdan M, McDonald RC. Mechanisms of membrane degradation. Ibid 2003;3:648.
[113] Shi M, Anson FC. Dehydration of protonated Nafion® coatings induced by cation exchange and monitored by quartz crystal microgravimetry. J Electroanal Chem 1997; 425(1–2):117–23.
[114] Inaba M, Kinumoto T, Kiriake M, Umebayashi R, Tasaka A, Ogumi Z. Gas crossover and membrane degradation in polymer electrolyte fuel cells. Electrochim Acta 2006;51(26):5746–53.
[115] Hamada AS, Karjalainen LP, Somani MP. Electrochemical corrosion behaviour of a novel submicron-grained austenitic stainless steel in an acidic NaCl solution. Mater Sci Eng A 2006;431(1–2):211–7.
[116] Lü AQ, Zhang Y, Li Y, Liu G, Zang QH, Liu CM. Effect of nanocrystalline and twin boundaries on corrosion behavior of 316L stainless steel using SMAT. Acta Metall Sin (English Letters) 2006;19(3):183–9.
[117] Wang XY, Li DY. Mechanical and electrochemical behavior of nanocrystalline surface of 304 stainless steel. Electrochim Acta 2002;47(24):3939–47.